TD-02-017
05 /02

CONCEPT OF THE FIRST VLHC PHOTON STOP CRYOGENIC DESIGN EXPERIMENT

P. Bauer, C. Darve*, K. Ewald, P. Limon, T. Nicol
Fermilab, Technical Division
*Fermilab, Beams Division

As part of Fermilab's recent Very Large Hadron Collider (VLHC) feasibility study, a water-cooled photon stop was proposed as a possible device to intercept the intense synchrotron radiation in the high field stage VLHC with minimal plug-power. The photon stop, if feasible, promises not only significant savings in cooling power compared to a solution in which the synchrotron radiation is extracted from a beam screen at cryogenic temperatures, but also virtually removes the synchrotron radiation limitation to beam energy and luminosity in a future VLHC.
Among the technological challenges regarding photon stops is their cryo-design. The photon stop is water-cooled and operates in a cryogenic environment. A careful cryo-design is therefore essential to enable operation at minimum heat transfer between the room temperature sections and the cryogenic parts. A photon stop cryo-design was developed and is being presented here. An experiment, presented in this note, is being prepared that will allow verification of the thermal model and the proposed cryo-design.

1) INTRODUCTION

A very large hadron collider (VLHC) is being proposed as a possible successor to the large hadron collider (LHC). The latest set of general characteristics of the second stage of this machine, as recently studied [1], is listed in Table 1. The second stage VLHC, referred to as VLHC2 in the ongoing text, will produce protons at energies more than 10 times larger than the LHC. Unlike the first stage, the VLHC2 beams will emit considerable synchrotron radiation power, when steered through the high field magnets.

Energy per proton E_p @ collision(TeV)	87.5
Gamma γ	93284
Peak luminosity L ($cm^{-2}s^{-1}$)	$2 \cdot 10^{34}$
Total circumference C (km)	233
Arc bending radius ρ (km)	29.9
Dipole field B @ collision (T)	9.7
Number of bunches N_b	37152
Initial Nr. of protons per bunch $N_{p/b}$	$7.5 \cdot 10^{9}$
Initial beam current I_b (mA)	57.4
Bunch spacing t_b (ns)	18.8
Radiation damping time τ_R (hrs)	2.5
Revolution frequency f_0 (Hz)	1286
Normal. (round) beam emittance ε_N @ collis. (rms) (mm-mrad)	$0.08 \cdot \pi$

Table 1: VLHC2 machine parameters [1].

The synchrotron radiation power radiated by the stage 2 beam, calculated with the parameters of Table 1, is listed in Table 2 together with the other synchrotron radiation characteristics. A more detailed description of the calculations is given in [2],[3]. The synchrotron radiation power in this particular VLHC2 scenario amounts to ~5 W/m per beam.

Synchrotron radiation power per m, per beam (W/m)	4.7
Critical energy E_{crit} (keV)	8.03
Number of incident photons per meter Γ ($m^{-1}s^{-1}$)	$1.2 \cdot 10^{16}$
Incidence angle of synchrotron radiation (mrad)	1.31
Azimuthal (rms) width of synchr. rad. strip on beam tube / photon stop* (mm)	0.5
Radial (rms) width of synchr. rad. strip on the photon stop* (mm)	10

Table 2: Synchrotron radiation parameters in the VLHC2. *Calculated for 14 m long magnets and 3 m long magnet inter-connects.

The synchrotron radiation power in the VLHC2, with the operational parameters listed in Table 1, is ~50 times larger than in the case of the LHC. The cost at the plug for removing this synchrotron radiation heat load from low temperature surfaces is considerable. A more detailed discussion of the cooling issues is given in [4], [5], [6]. The plug power requirement for extracting the synchrotron radiation heat load can be significantly reduced by photon stops operating at room temperature. Photon stops

(Figure 1) are water-cooled absorbers that protrude into the beam tube at the end of each bending magnet and scrape off the synchrotron light beam emitted in the second magnet up-stream from their location. Radiation fan geometry and cooling requirements demand a certain minimum photon stop surface area [7]. To increase the cooling surface area and reduce reflectivity, the absorber uses a wedge-shaped cavity to trap the synchrotron radiation light beam. The synchrotron radiation power deposited on the photon stop in a VLHC2 is of the order of 100 W. The shape of the photon stop mainly responds to stipulations regarding its impedance. A detailed discussion of the impedance related implications of the photon stop and the results of numerical impedance calculations are reported elsewhere [8]. The general implications of photon stops for VLHC's are discussed in [9]. A first photon stop prototype was designed and manufactured (Figure 1).

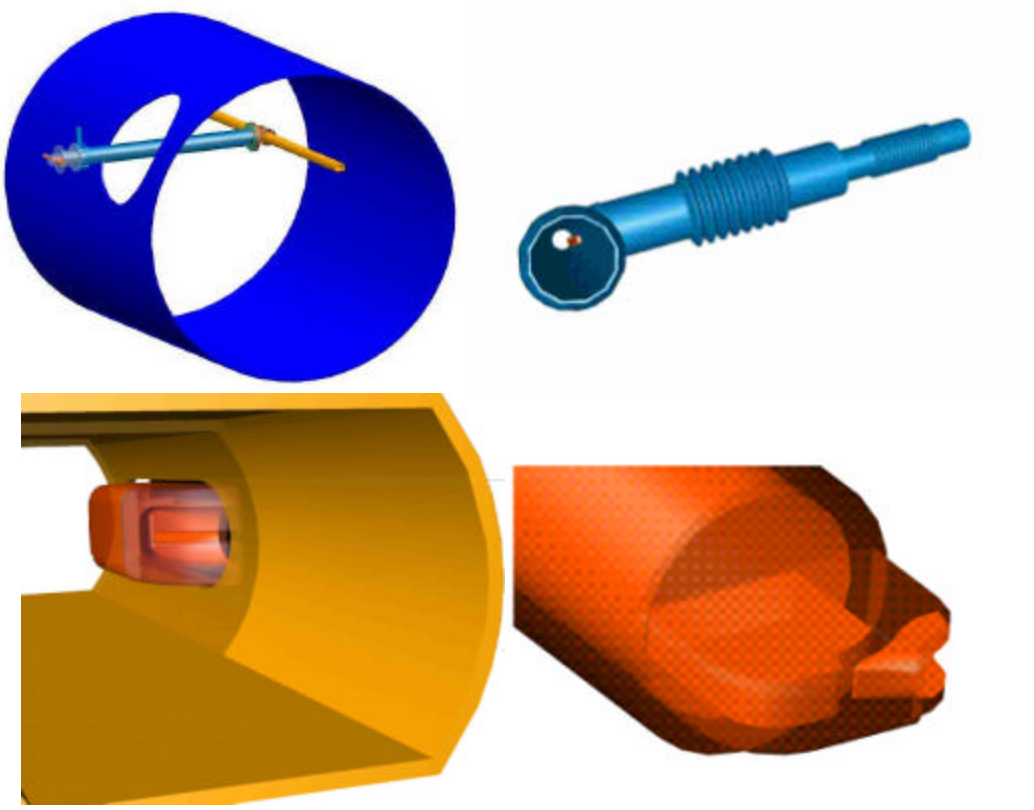

Figure 1: Conceptual design of the VLHC photon stop: illustration of assembly in magnet interconnect (upper left), cryo-module assembly (upper right), close-up on absorber in beam tube (lower left), endpiece - absorber (lower right).

Figure 1 shows a conceptual sketch of a complete photon stop assembly in the accelerator magnet interconnect. A beam screen and the outer cryostat jacket are shown. The photon stop insert, i.e. the part containing the cooling pipes and the radiation absorber, is at room temperature or above, while the environment is at cold-mass (~4.5 K) or beam screen (~100 K) temperatures. The absorber enters the beam screen through a rectangular hole from the side. To limit the thermal interference and thus minimize thermal losses, an optimal cryo-engineering design is crucial. To test the cryo-design, experiments should be conducted in a magnet interconnect mock-up, consisting of a vacuum vessel, a 4.2 K

bore and a tube cooled by a helical LN_2 heat exchanger representing the high temperature beam-screen. The complete photon-stop cryo-assembly will be mounted into the vacuum vessel in the same way it would be in the magnet interconnect cryostat in an accelerator. The heat transfer between the cold tube and the warm photon stop, i.e. the thermal loss rate, can be measured with an array of temperature sensors, mounted on various sections of the photon stop and via a measurement of the cryogen boil-off rates. The synchrotron radiation heating will be simulated with an electrical heater mounted to the tip of the photon stop. This experiment would as well allow us to investigate the risk of freezing in the cooling water lines in the absence of synchrotron radiation heating. The cryo-design, the cryo-design calculations and the concept of a first cryo-test of the photon stop prototype will be discussed next.

2) PHOTON STOP / BEAM SCREEN ASSEMBLY DESIGN FOR CRYO-TEST

2.1) Introduction

A first pass engineering design of the photon stop for the VLHC study was presented in [7]. The design has evolved since to address some key issues such as vacuum and HOM trapping. One of the major new elements of the design was the introduction of an intermediate, so-called inner shield (~80 K) to thermally shield the 4.2 K environment from the room temperature parts of the photon stop. Another major design change is that the design assumes a large cold bore OD (~80 mm), which is ~2 times the VLHC2 coil aperture. This design change considerably facilitates the cryo-assembly, because the outer shield can be welded directly to the cold-bore tube with no need for diameter-adaptors. Figure 2 shows a cut through the photon stop cryo assembly model. The cryo assembly consists of the water cooled radiation absorber in the center, surrounded by an inner and an outer shield. The cryo-assembly as well includes a 60" long dummy beam screen / cold bore section. The 1.5" ∅ dummy beam screen is cooled to ~80 K, while the cold bore is cooled to ~4.5 K. The core of the photon-stop is inserted into the inner thermal shield, which is made from a 1.5" ∅ tube, actively cooled to ~80 K throughout the bottom half, and negotiating a temperature drop from room temperature to ~80 K through a long bellows along its upper portion. The lower, 80 K, part of the inner shield in turn is surrounded by a 3"∅ outer shield, which, through a similar bellows, negotiates a temperature drop from ~80 K at its top to ~4.5 K at the bottom, where it is welded to the 3"∅ cold bore.

To facilitate the temperature control the dummy beam screen and cold bore tubes are made of copper. For the sake of simplicity, the inner and outer shield tubes are made from copper as well. The bellows with their flanges are made of stainless steel. The bellows are fixed to the shield tubes through mixed steel/copper flanges. The photon stop insert is made from copper entirely (except for the water tubes) and uses a simplified design, consisting of a copper tube with a radiation absorber mock-up welded to its end. Other simplifying design elements, that would not be permissible in a real accelerator setting, is the use of mixed material flanges (not vacuum tight) and a water to vacuum weld at the photon stop tip. The former would not be an issue in a real accelerator setting in which all parts would be made from steel. The latter can easily be avoided. A detailed view of the center of the photon stop cryo-test assembly is shown in Figure 3.

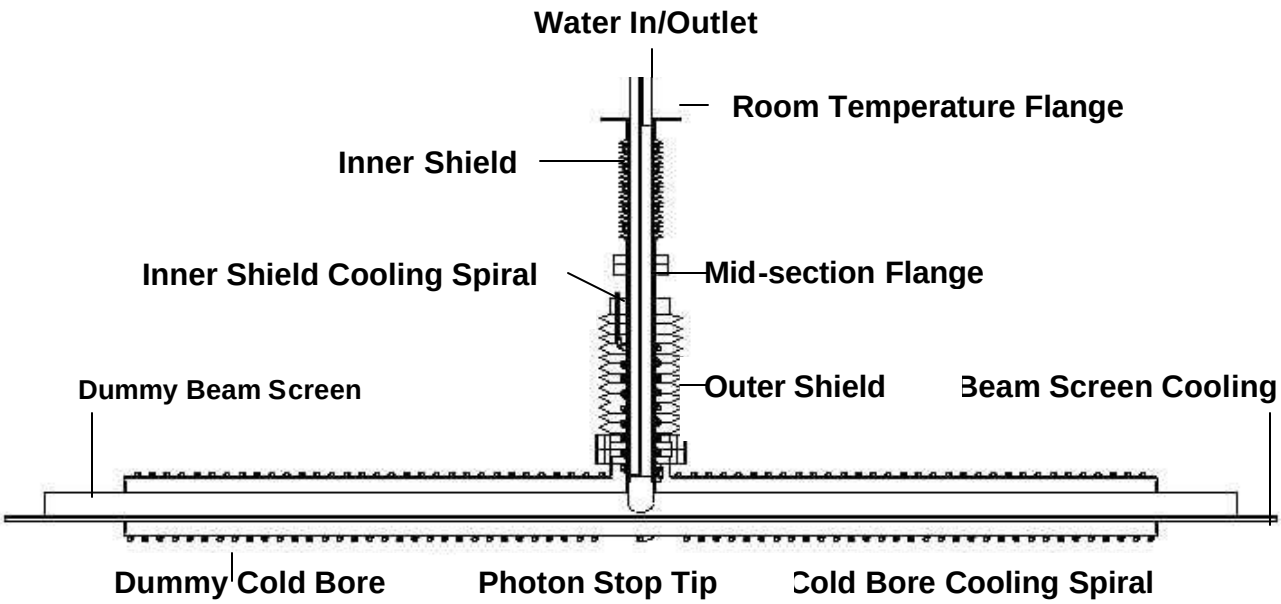

Figure 2: Cut through photon stop cryo-test assembly.

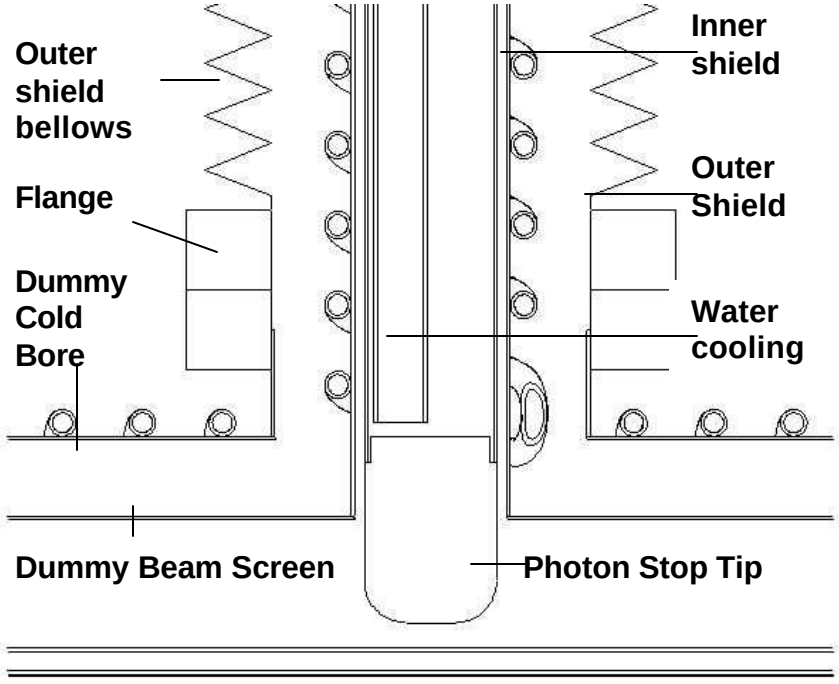

Figure 3: Cross-section through photon stop assembly for cryo-testing, detail.

2.1) Absorber

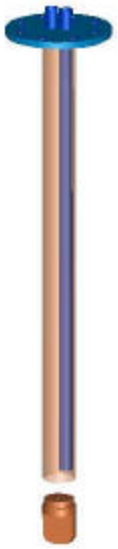

Figure 4: Photon stop insert.

Unlike an accelerator compatible photon stop design, the cryo-test photon stop will be simpler because of reduced concern regarding possible water leaks. The absorber insert, shown in Figure 4, consists of a 1.25" ∅, 19.75" long copper tube, welded at one end to the absorber and at the other end to a disc with two holes for the 0.5" ∅ stainless steel water tubes (0.03" wall thickness). The brazing between the copper tube and the bottom absorber would not be permissible in a real accelerator setting. At the top the copper tube is closed up by a disc, containing two holes for the water tubes. The stainless steel disc will be gold-brazed to the copper tube. In addition, the simplified cryo-test version of the absorber does not include a cavity to reduce reflectivity. Three press-fitted G10-pins, placed at 120 degrees around the bottom of the absorber will serve to center the absorber within the inner shield tube with minimum heat transfer. The pins are not shown in Figure 4.

2.2) Inner Shield

The photon stop thermal shield (so called "inner shield") has to negotiate a temperature drop from ambient to 100 K (or less) and absorb the thermal radiation from the 300 K insert in its core. To shield the cryogenic environment from the room temperature radiation, the shield is assembled around the water cooled photon stop insert. Figure 5 shows a sketch of the inner thermal shield. The shield consists of a 1.5" ∅ copper tube (wall thickness=0.03") with a brazed copper cooling spiral as the lower part and a stainless steel bellows (with flanges) as the top part, connected by a mixed steel/copper flange. At the bottom the inner shield is welded to the 1.5" ∅ dummy beam screen. At the top end the shield is at room temperature and bolted to the top flange of the water-cooled photon stop. The upper part of the inner shield is not surrounded by any outer shield. A 7.25" long stainless steel bellows negotiates the temperature drop from ambient at the top to ~80 K in the middle by increasing the thermal length. It also provides

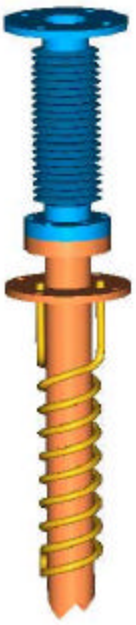

Figure 5: Inner thermal shield.

mechanical flexibility and therefore facilitates assembly and system alignment. The lower section of the inner shield is thermalized at the beam screen temperature of ~80 K with a cooling spiral made from copper tubing. In the cryo-test the spiral will contain LN_2, whereas in a VLHC it would contain GHe from the cold-mass thermal shield. The LN_2 cooling system enters the shield through the brazed copper flange and spirals down along the inner shield tube. The cooling spiral is brazed to the inner shield tube to improve the thermal contact. The spiral pitch is 0.75", the copper cooling tube ∅ is 0.25" (0.03" wall thickness). The brazed copper flange connects (and thus thermalizes) as well the inner shield to the outer shield, which ends in the 80 K mid-section. At the bottom the inner shield tube passes through a hole in the cold-bore tube and is welded to the 1.5" ∅ dummy beam screen. In the cryo-test assembly the inner shield cooling spiral does not wind around the beam-screen. Instead, a separate LN_2 cooling tube is brazed to the beam screen tube from the inside (see Figure 7).

2.3) Outer Shield

Figure 6: Outer shield.

The outer thermal shield (Figure 6) is made from a 3"∅ copper tube, stainless steel flanges and a stainless steel bellows. It is bolted to the copper flange on top and is welded to the cold bore at the bottom. This copper flange is welded to the inner shield. A 7.25" long stainless steel bellows negotiates the temperature drop from ~80 K at one end to the cold-bore temperature (~4.5 K) at the other end. To prevent a copper/steel weld the steel bellows is fixed at the top and bottom via flanges. At the top the bellows are bolted to the inner shield copper flange, which in turn is welded to the inner shield. This flange is as well crossed by the LN_2 tubing for the inner shield cooling. In the cryo-test assembly the cold bore tube OD is 3", such that a straight-forward brazing between outer shield and the dummy cold bore tube is possible.

2.4) Beam-Screen Assembly

The 60" long dummy beam screen (copper) tube (1.5" ∅) is inserted into the dummy cold-bore (copper) tube (3" ∅), supported with G10 spiders at both extremities. A schematic of the beam-screen assembly is shown in Figure 7. The spider is shown separately in Figure 8. The cold-bore tube is cooled from the outside by a 0.75" pitch, 0.25" ∅ cooling tube spiral with LHe flow. In the cryo-test assembly the inner tube (beam screen) is maintained at LN_2 temperature with a copper cooling duct welded to it along its entire length. The spider, which is a critical part of the cryo-design, is the only mechanical connection between the 80 K and 4.2 K systems.

Figure 7: Beam-screen / cold-bore assembly.

One spider of the type shown in Figure 8 will be installed at each extremity of the dummy beam screen assembly. As will be shown in part 3), thermal model calculations indicate that a spider of the type shown in Figure 8 restricts the 80 K to 4.2 K heat flux to less than 0.43 W. The spider thickness is 0.1875", the three contact pins are 0.125" (0.3"?) wide.

2.5) Test Cryostat

Figure 8: G10 spider.

The photon stop assembly could be installed into an existing cryostat, shown in Figure 10. The cryostat is 62" long, 17" in diameter (although only the inner 14.75" of diameter are accessible because of the cryostat thermal shield) and has a large vertical access window (with a diameter comparable to the cryostat tube). The photon stop cryo-assembly will be mounted into the cryostat with spiders, such as shown in Figure 12. The detailed assembly procedure is outlined in 2.6). The lines for the LHe, LN_2 and cooling water circuits are not explicitly shown. The helium transfer lines enter the cryostat through the top access window. Water and LN_2 circuits enter through the small side-ports in the middle of the cryostat. The cryogens as well as the water will be directed to the connection ports on the photon stop / beam screen assembly with copper tubing. VCO fittings will be used to connect the tubes to the ports. The pipes within the cryostat will be equipped with union fittings in order to facilitate the assembly and disassembly of the system. The wiring of the temperature sensors and heaters will be routed through the lateral windows in the cryostat mid-section. The LHe will be provided from dewars. A flow diagram is given in Figure 13.

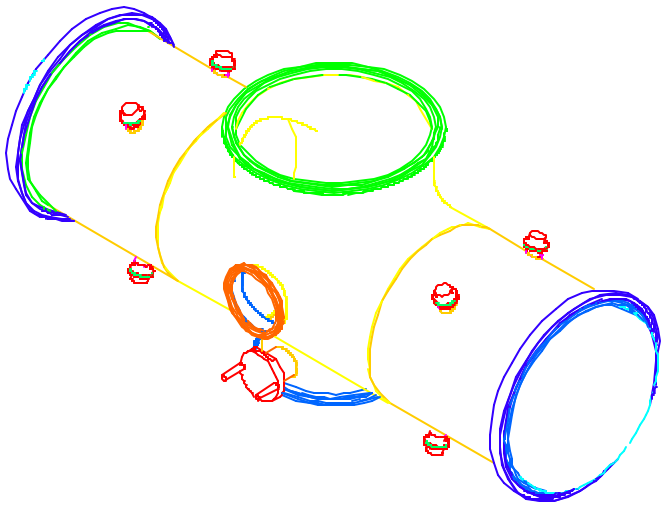

Figure 10: Cryostat for photon stop testing.

2.6) Photon Stop Cryo-Test Assembly Procedure

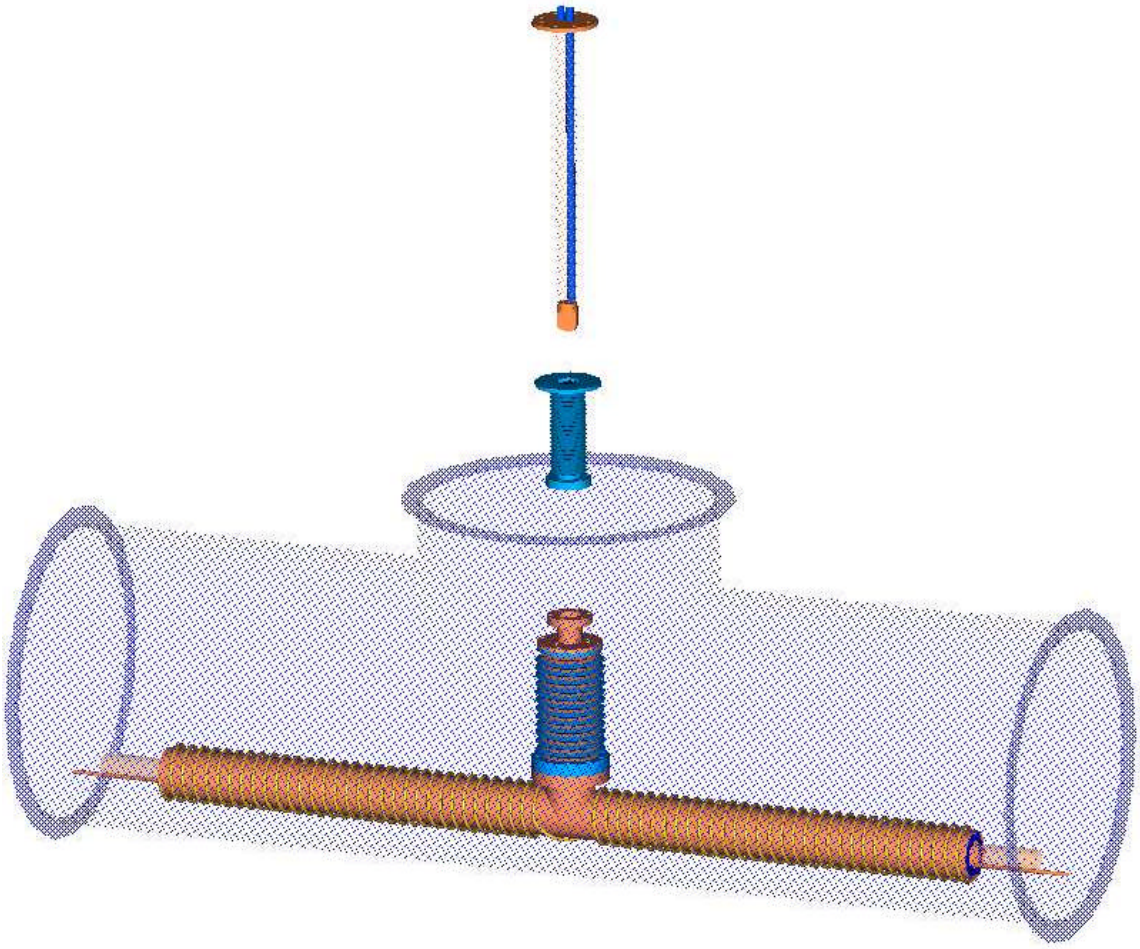

Figure 11: Schematic showing how photon stop is assembled into cryostat thermal shield.

The photon stop assembly could be installed into the cryostat described in 2.5. The total weight of the assembly is approximately 25 kg. After soldering the cooling spiral to the cold bore tube and the straight cooling tube to the beam screen tube, the dummy beam screen is slid into the cold bore and supported with the G10 spiders in the ends (Figure 7). Then, the inner shield is assembled, that is, the copper flange and the cooling spiral are brazed to the inner shield tube. Before welding of the shield assembly to the dummy beam screen assembly, the outer shield (bellows) is bolted to the copper flange. Retracting the outer shield bellows, the inner shield can then be welded to the beam screen through the hole in the cold-bore tube. The next step consists in welding the outer shield to the cold-bore tube. Next, the beam screen / cold bore – inner / outer shield assembly is placed into the cryostat (Figure 11) and positioned with the large G10 spiders shown in Figure 12. The top part (bellows) of the inner shield can then be attached to the mid-section flange on the inner shield through the top access window of the cryostat

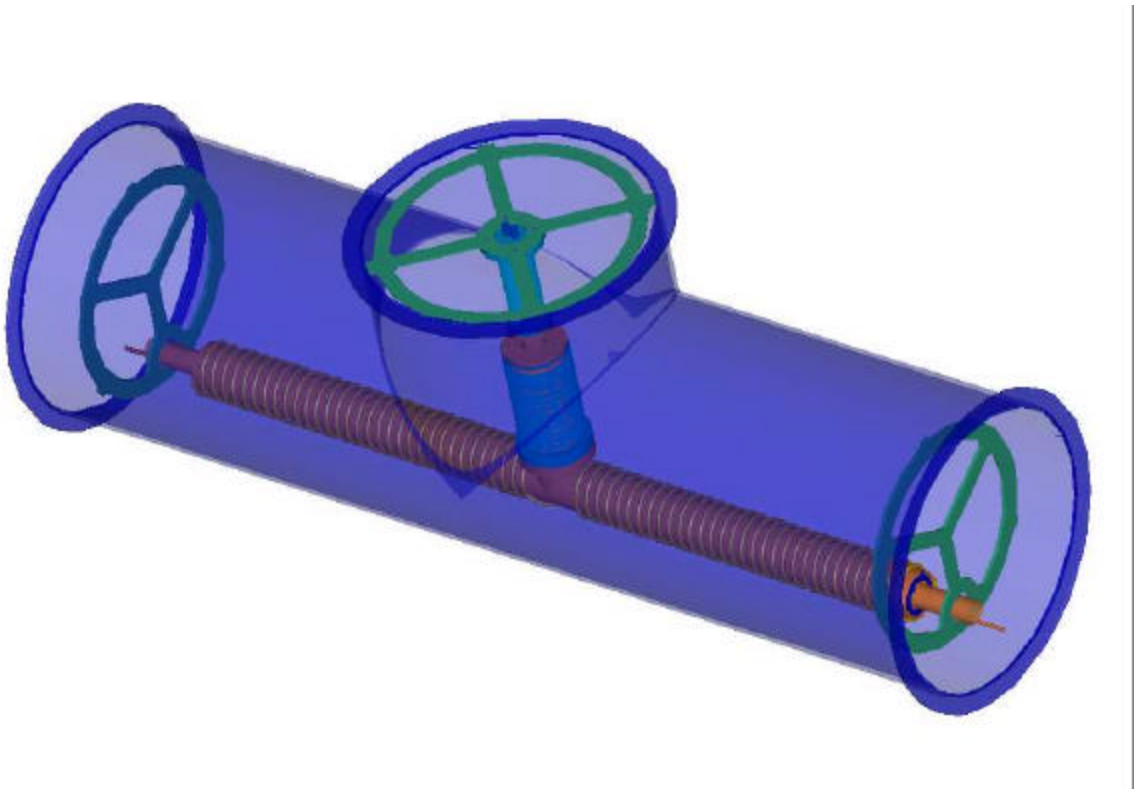

Figure 12: Schematic of photon stop cryo-test assembly in cryostat thermal shield.

(Figure 11). The photon stop insert is introduced into the inner shield and the inner shield bellows is bolted to the insert top flange. The top spider, which prevents the photon stop from tilting, is bolted to the top flange as well. The plumbing for the different cooling circuits (LHe, LN_2, H_2O) is then connected with flexible tubing. Finally the vacuum tight top-flange ("dome") and the side and end caps are put in place to seal the vacuum vessel.

3) MODEL CALCULATIONS

3.1) Introduction

The theoretical model allows to specify the thermo-mechanical design of the photon stop, to limit the heat load to the 4.5 K (dummy cold bore) and 77 K (shielding) temperature levels. In addition, the model allows to simulate dynamical conditions by adding heat loads and computing the ensuing changes of temperature. The model was used to support the design presented in 2). The theoretical model will be completed and validated during the experiment, which will provide temperature measurements in static and dynamic heat load conditions. Table 1 summarizes the photon stop design parameters and temperatures.

Temperature of the dummy cold bore (K)	5
Temperature of the dummy beam screen (K)	80
Temperature of the dummy (absorber) photon-stop (K)	300-350
Temperature of photon stop, inner shield (K)	80-300

Temperature of photon stop, outer shield (K)	5-80
Length of the vacuum vessel, dummy beam screen and cold bore (in)	60
Length of the bellows (in) (thermal length is twice longer)	7.5
Total length of the photon stop inner shield (in)	12.75
Total length of the photon stop outer shield (in)	8.5 (to check)
Length of the photon stop-absorber insert (in)	19.75

Table 3: Summary of the design parameters and temperatures.

The vacuum is estimated to 10^{-4} Pa. Materials considered are copper and stainless steel, their thermal and mechanical properties are taken from literature [10].

3.2) The LN_2 Temperature Level

There are three major components operating at LN_2 temperature in the photon-stop cryo-test set-up: the cryostat thermal shield, the photon stop inner shield and the dummy beam-screen. The cryostat thermal shield is mainly receiving thermal radiation from the outer, room temperature walls of the cryo vacuum-vessel. The photon stop inner shield absorbs mostly the thermal radiation from the water cooled, room temperature photon stop insert. The dummy beam screen absorbs some radiation from the ~350 K photon stop tip, where the synchrotron radiation heat load is absorbed (simulated by a heater in the cryo-test).
The vacuum vessel thermal shield consists of a copper shield, cooled with a LN_2 spiral and surrounded by a wrap of 30 layers of MLI. Radiation and conduction into residual gas need to be estimated. The conditions were similar in the LHC main magnet cryostat thermal model, therefore the calculation takes into account results of measurements performed on the LHC main magnet cryostat at CERN, [11]. Equation (1) relates the contribution of radiation and residual gas conduction to the heat load from room temperature to the 80 K cryostat thermal shield.

$$Q = A\left[a\left(\frac{T_v^2 - T_{ts}^2}{2} \right) + b\left(T_v^4 - T_{ts}^4\right) \right] \tag{1}$$

where $a=4.7\cdot10^{-6}$ W/m^2/K^2 and $b= 1.25\cdot10^{-10}$ W/m^2/K^4.

T_v and T_{ts} are the temperatures of the vacuum vessel (300 K) and the thermal shield (~80 K) respectively. The heat load calculated from the ambient to the cryostat thermal shield is 2.8 Watt (if we would consider no MLI wrap it would be 64.3 Watt).

The photon stop inner shield absorbs the thermal radiation from the water cooled, room temperature photon stop insert. The radiation heat load can be calculated from the Stefan-Boltzmann law ($\sigma=5.67\cdot10^{-8}$W/m^2/K^4) (2):

$$Q = e s S\left(T_{ps}^4 - T_{psts}^4\right) \tag{2}$$

With, e the emissivity and S the surface of the emitting object. The heat load on the inner shield due to the radiation from the photon stop insert is 3.6 W.
The photon stop insert is not free-floating within the inner shields, rather it is spread from the shield through a guiding support consisting of three G10 pins, 2 mm in diameter, press-fitted into the nose-piece (at the bottom) of the photon stop insert. The annular gap between the insert and the inner shield is 1.65 mm. The heat load via conduction from the absorber to the inner shield is less than 1 W.
The conduction heat load through the inner shield top bellows (7.25" length, 0.03" wall thickness, thermal length enhancement factor 2) from ambient to the 80 K level is only 60 mW.
The radiation heat load from ambient to the beam screen tip is negligible given the small emitting surface area.
The total static heat load on the LN_2 system is thus expected to be ~4.61 W.

3.3) The LHe Temperature Level

The photon stop cryo-test design uses a tube with a LH_2 cooling spiral to simulate the magnet cold-bore. The heat loads by radiation from the 80 K cryostat thermal shield and the ~ 80 K dummy beam screen to the cold bore, calculated with Stefan-Boltzmann, are 75 and 25 mW, respectively. The radiative heat transfer from the vacuum vessel axial end-cap is less then 0.2 W.
The largest heat load to the LH_2 system is a result of conduction from a) the dummy beam screen and outer shield to the cold bore via the support spiders shown in Figure 8 and b) the photon stop outer shield bellows. The heat load by conduction is calculated with the Fourier equation:

$$Q = \int_{T_{cold}}^{T_{warm}} k_{G10}(T)dT \frac{A}{L} \qquad (3)$$

where A and L are the cross-sectional area and thermal length of the heat transfer element (the G10 spider or stainless steel bellows). The ratio of G10 / steel thermal conductivity assumed is 3.5 at 5 K, [10].
The thermal length and the cross-sectional area of the G10 spider were optimized in order to limit the conduction. The objective was to limit the heat load to less then 0.3 W. The thickness / width of the spider support therefore is 0.1875 mm / 0.33 mm. In order to limit the conduction from the photon stop inner thermal shield to the dummy cold bore through the outer shield stainless steel bellows (and copper "adaptor"), the bellows thermal length / wall thickness was specified to be 14.5" / 0.03" mm. This heat load can increase considerably in case the middle flange is not at 80 K. If the bellows is at 300 K this heat load can increase up to 1.2 W. The bellows heat load is thus reduced to less than 0.15 W. Hence the 5 K dummy cold bore receives a total of less than 1 W (less than 2.2 W in the worst case).

4) PHOTON STOP CRYO-TEST PLAN

4.1) Experimental Model and Instrumentation

The goal of the test campaign are to 1) check the feasibility of the current photon stop cryo design, 2) measure the contribution of the different components to the system heat load, 3) validate the model used to predict the heat loads for various conditions, 4) check the distribution of the temperature at various points of interest. A flow diagram for the cryogenic circuits is shown in Figure 13.
The heat load to the liquid helium and liquid nitrogen temperature levels will be determined by the heater technique. This technique uses the measurement of a temperature change along the cooling duct as a result of a heater power Q_{el} applied to the cooling duct, according to the heat balance equation (4).

$$Q_{el} + Q_0 = \dot{m} C_p \left(T_{out} - T_{in}\right) \tag{4}$$

The linearity of this relation allows extrapolation to $\Delta T=0$, in which case the factor Q_0, the static heat load can be determined. Various accelerator load configurations are simulated by an electrical heater mounted to the absorber tip. The heater technique will be used to determine the resulting heat loads on each of the components for varying heat load on the absorber.
The instrumentation (see flow diagram in Figure 13) is mainly composed of Cernox and Platinum temperature sensors mounted with Stycast to the piping (vacuum side). 4 Cernox are mounted at each extremity of the copper cooling spiral of the dummy cold bore tube. Since this measurement is of prime importance, the sensors are duplicated. In addition, eight PT102 temperature sensors are mounted at each extremity of the cooling system of the photon stop thermal shield, cryostat thermal shield and dummy beam screen and photon stop insert (water circuit). To improve the accuracy of the measurement a flow-meter will be provided for the LHe circuit.
Heaters are made of Nickel wiring encapsulated in Kapton foils. They are fixed with STYCAST to the LHe and LN_2 piping loops, on the vacuum side. Appropriate heaters are located along the dummy beam screen and at the absorber extremity. A specific attention is driven by the contact between the heater and the piping. Heaters are located also around and in the water loop in order to prevent freezing.
Pressure transducers are available in the A0 North LHe supply system.
The wires of each sensor which are located in the vacuum space are routed to the lateral exit ports of the cryostat. Maganin wires are preferred in order to limit the load to the sensors and cold media. The thermometry technique and the 19-pins connectors are similar to these used for LHC thermal model [13]. The connectors are welded to the flanges and transfer the signal to the DAQ system. The instrumentation measurement are read-out with a scanner / multimeter system available at the TD. An existing Labview program can be modified for the DAQ.

A tentative program could be:

1- Installation and commissioning of the cryo-test and DAQ
2- Measurement of the A0 North cave (or other test stand) capacity

3- Measurements of the static heat leaks and temperature distribution
4- Measurements of effect of heating on photon stop tip

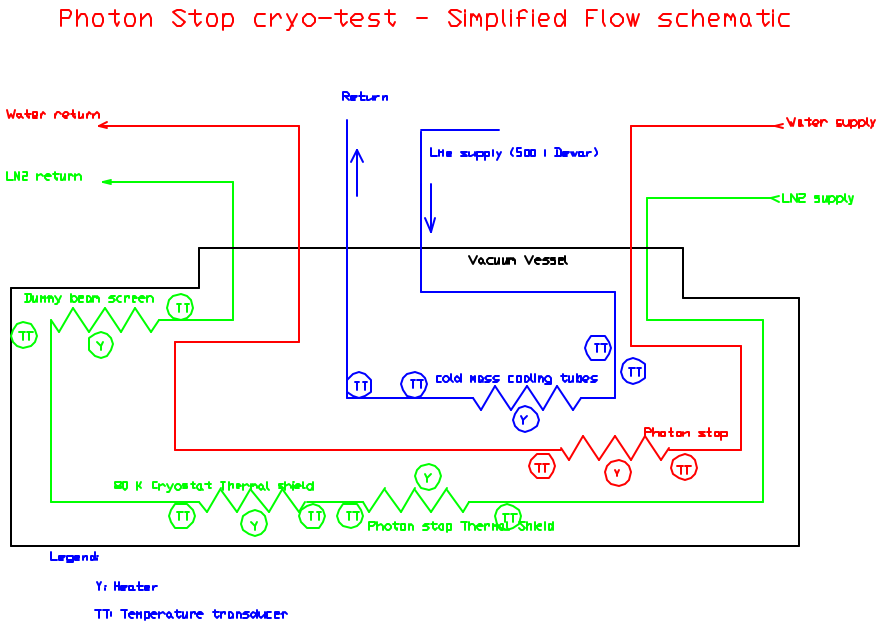

Figure 13: Flow schematic and connection flanges for cryogenic fluid circuits.

4.2) Schedule

The schedule is partially constrained by the necessity to free the test cryostat before fall 2002. Therefore the test campaigns are planned for summer 2002. The design and update of the test cryostat, is estimated to take one month. The procurement, production and assembly of the cryo design component will have to be completed within 2 months. Drawings can be finalized in 2-3 weeks. The installation and the test itself will be conducted in the A0 North cave facility, if possible.

4.3) Cost Estimate

Estimated Total ~ $ 8,500 (not including assembly labor).

Table 4: Cost estimate for photon stop cryo-experiment.

#	Item Description	Price/ Qty ($)	Qty	Price total ($)
	Mechanical			
1	¼" copper tubing for heat exchanger (80 ft min) and piping (80 ft min)	0.5/ft	200 ft	100
2	½" stainless steel tubing for water pipes (80 ft min)	0.23/ft	80 ft	18.4
3	1,5" copper tube, inner shield, dummy beam screen		10 ft	200

4	3” copper tubing, outer shield, dummy cold bore		10 ft	250
5	1¼” copper tubing, photon stop insert		X ft	100
6	1¼” solid copper billet		X ft	50
7	1½” ∅ bellows (7.5“ long) with 2.75/4“ flanges bottom/top, how-about MDC ?		1	300
8	3” ∅ bellows (7.5“ long) with 4“ flanges top/bottom how-about MDC ?		1	400
9	4” ∅ copper billet for 3 flanges, (outer shield - bottom & top, insert - top)	?	1.5”	50
10	2.75” ∅ copper billet for inner shield mid-section flange	?	5/8”	50
11	G10 for 3 large spiders, ¼” thick, 14” ∅		3	50
11	G10 for 2 small spiders, 3/16” thick, 3” ∅		2	10
12	Water flange, 6” OD, with H_2O 2-way feed-through, 2x19 wires feed-through	80	1	100
13	LN_2 flange, 6” OD, with LN_2 2-way feed-through, 2x19 wires feed-through	80	1	100
14	Bulkhead SS-4-VCO-61 LN_2-loop	11.5	4	46
15	Socket weld gland SS-4-VCO-3 LN_2-loop	1	15	15
16	Gasket SS-4-VCO-2 GR LN_2-loop	1	15	15
17	SS nut SS-4-VCO-1 LN_2-loop	4	4	16
18	Union Gasket SS-4-VCO-2 GR LN_2-loop	1	15	15
19	Union SS nut SS-4-VCO-4 LN_2-loop	5	4	20
20	Union body socket weld conn. SS-4-VCO-1 LN_2-loop	5	8.25	41
21	Bulkhead SS-8-VCO-61 H_2O-loop	11.5	4	46
22	Socket weld gland SS-8-VCO-3 H_2O loop	1	15	15
23	Gasket SS-8-VCO-2 GR H_2O loop	1	15	15
24	SS nut SS-8-VCO-1 H_2O-loop	4	4	16
25	Union Gasket SS-8-VCO-2 GR H_2O loop	4	1	4
26	Union SS nut SS-8-VCO-4 H_2O loop	2	4	8
27	Union body socket weld conn. SS-8-VCO-1 H_2O loop	2	8.25	16
28	Bulkhead SS-8-VCR-61 LHe-loop	11.5	2	23
29	Socket weld gland SS-4-VCR-3 LHe-loop	1	4	4
30	Gasket SS-4-VCR GR LHe loop	1	4	4
31	SS nut SS-4-VCR-1 LHe-loop	2	4	8
32	Union Gasket SS-4-VCR-2 GR LHe-loop	4	1	4
33	Union SS nut SS-4-VCR-4 LHe loop	2	4	8
34	Union body socket weld conn. SS-4-VCR-1 LHe loop	2	8.25	16
35	SS Flange for return adaptor OD 2 3/16 LHe loop	1	16	16
36	1½” OD, #810-61 Bulkhead Union	12	2	24
37	1¼” OD, #401-PC Port Connector	4	20	80
38	1½” OD, #811-PC Port Connector	4	20	80
39	1¼” OD, #400-6 Union	0.83	10	83
40	1½” OD, #810-6 Union	0.83	10	83
41	¼“ tubing strap #9434T13	1	20	20
42	½” Screw socket, #6-32 to bolt flanges, enough?	0.25	20	5

43	Screw socket MA-364149 M3x6mm, R.H.M.S.	0.2	20	10
44	Screw socket HD SS #6-32 x 0.5"	0.25	20	5
	Sum Mechanical			2470
	Labor ($ 70/hr)			
45	Photon Stop insert	70	4	280
46	G10 Spiders	70	6	420
47	Beam Screen	70	3	210
48	Cold Bore	70	1	70
49	Heat Exchangers	70	4	280
50	½" stainless steel tubing ????	70	2	140
51	Cu Flanges	70	10	700
52	Plumbing	70	7	500
53	Welding	70	12	840
	Sum Labor			3430
	Instrumentation			
54	PT102, temperature sensor	72	8	576
55	CX-1050-SD, temperature sensor	156	4	624
56	Stycast 2850 FT	165	2	330
57	150 Watt Heater	29	7	203
58	Manganin wire	1/ft	20 ft	20
59	Connectors, 19 pin female	19	4	76
60	Connectors, 19 pin male	19	4	76
61	O-rings #2-021	0.2	20	10
62	Doppler flowmeter	600	1	600
	Sum Instrumentation			2540

References:

[1] P. Limon et al., "*Design Study for a Staged Very Large Hadron Collider*", Fermilab-TM-2149, June 2001.

[2] M. Pivi, W.C. Turner, P. Bauer, P. Limon, "*Synchrotron Radiation and Beam Tube Vacuum in a Very Large Hadron Collider, Stage 1 and Stage 2*", Proceedings to the Particle Accelerator Conference 2001, Chicago, Sept. 2001

[3] P. Bauer et al., "*Synchrotron Radiation Issues in the VLHC*", Proceedings to the Particle Accelerator Conference 2001, Chicago, Sept. 2001

[4] P. Bauer, C. Darve, I. Terechkine, "*Synchrotron Radiation Issues in Future Hadron Colliders*", to be published in the proceedings of the 2001 Particle Physics conference at Snowmass

[5] P. Bauer, C. Darve, I. Terechkine, "*Synchrotron Radiation Issues in Future Hadron Colliders*", Summary of the contributions to the T2 WG at the Snowmass 2001 conference, Fermilab, Technical Division note TD-01-061, August 2001

[6] C. Darve et al: "*VLHC beam-screen cooling*", Fermilab, Technical Division Note TD-01-005, Feb. 2001

[7] P. Bauer et al. "*A Photon Stop for the VLHC-2, Engineering Design 1*", Fermilab, Technical Division note, TD-01-023, April 2001

[8] N. Solyak, "*Photon stop for the VLHC-2 – Impedance Calculations*", Fermilab, Technical Division Note TD-01-014

[9] P. Bauer et al., "*Accelerator Physics and Technology Limitations in Stage II – type Very Large Hadron Colliders*", Summary of the contributions to the M4 WG at the Snowmass 2001 conference, Fermilab, Technical Division note, TD-01-062, October 2001

[10] Institute International du Froid / IIR, "*Les techniques de l'ingenieur*".
[11] C. Darve et al, "*Thermal performance measurements for a 10 meter LHC dipole prototype (Cryostat Thermal Model 2)"*, CERN, LHC-Project-Note-112, November 1997.
[12] C. Darve et al, *"Measurements of temperature on LHC thermal models*", Cryogenics Vol 41, Issues 5-6.